Multicomponent Combinatorial Development and Conformational Analysis of Prolyl Peptide–Peptoid Hybrid Catalysts: Application in the Direct Asymmetric Michael Addition

Alexander F. de la Torre,[†] Daniel G. Rivera,*[,†,‡] Marco A. B. Ferreira,[†] Arlene G. Corrêa,[†] and Márcio W. Paixão*[,†]

[†]Departamento de Química, Universidade Federal de São Carlos, São Carlos, SP 13565-905, Brazil
[‡]Center for Natural Products Study, Faculty of Chemistry, University of Havana, Zapata y G, 10400 La Habana, Cuba

S Supporting Information

ABSTRACT: A solution-phase combinatorial approach based on the Ugi four-component reaction was implemented for the development of new prolyl peptide–peptoid hybrid catalysts. Three different elements of diversity were varied during the creation of the set of catalysts: the amine, oxo, and isocyano components. The multicomponent nature of this process enabled the straightforward generation of a series of peptide–peptoid hybrids having the generic sequence Pro-N-R^1-Xaa-NHR^3, with Xaa being either Gly (R^2 = H) or Aib (R^2 = gem-Me) and R^1 and R^3 either alkyl or amino acid substituents. The catalytic behavior of the peptide–peptoid hybrids was assessed in the asymmetric conjugate addition of aldehydes to nitroolefins, where most of the catalysts showed great efficacy and rendered the Michael adducts with good to excellent enantio- and diastereoselectivity. A molecular modeling study was performed for two distinct catalysts aiming to understand their conformational features. The conformational analysis provided important information for understanding the remarkable stereocontrol achieved during the organocatalytic transformation.
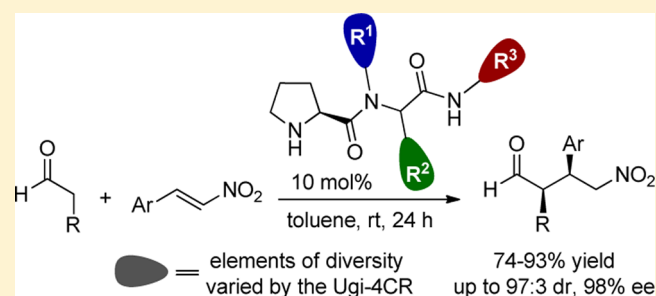
INTRODUCTION

The pursuit of novel chiral molecules for applications in metal-free asymmetric catalysis has inspired intensive research activity in the past decade. This massive effort has resulted in the discovery of several efficient organocatalysts for highly enantio- and diastereoselective organic reactions as well as cascade reaction sequences.[1] Among them, an important class of organocatalysts is that composed of oligopeptidic scaffolds, which have found remarkable applications in a wide range of catalytic asymmetric transformations such as acylation, oxidation, ester hydrolysis, Aldol reaction, conjugate addition, etc.[2] Although rational design plays an important role in the discovery of organocatalysts, further optimization steps are usually required, including variation of the nature and position of substituents around the chiral motif. In such a lead-catalyst optimization stage, combinatorial chemistry frequently plays a pivotal role because of its capacity to efficiently produce and screen hundreds of substances in a massive, parallel manner.[3] This strategy has been crucial in peptide catalyst discovery and development,[2,3] mainly because of the great advances in solid-phase combinatorial synthesis and high-throughput screening of peptide libraries.

However, a different scenario shows up in solution-phase approaches for organocatalyst development, as these latter are less straightforward and thus require a much higher synthetic effort in the preparation of compound libraries for catalytic activity screening. A solution for this may be the utilization of multicomponent reactions (MCRs),[4] i.e., one-pot procedures that incorporate at least three starting materials into a single structure. MCRs are almost unrivaled approaches in terms of chemical efficiency, atom economy, and diversity generation.[5] Hence, their utilization is of high incidence in drug discovery and development strategies based on the production of hetero- and polycyclic scaffolds, whereas the number of relevant hits can be significantly increased by taking advantage of the diversity-oriented character of such transformations.[6] However, despite the fact that the discovery of new catalysts can be approached in a similar way as drug discovery, the interest of the catalysis community in MCRs does not yet reflect the proven impact of such processes in other important areas such as medicinal[6] and natural products chemistry.[7]

Among the different types of peptide catalysts, those having proline at the N-terminus are especially suitable for both enamine and iminium ion activation. In a series of recent reports, Wennemers and co-workers used a combination of rational design and combinatorial chemistry to develop tripeptides based on the generic structure Pro-Pro-Xaa (where Xaa is an acidic α-amino acid).[8] Thus, the so-called Wennemers catalyst D-Pro-Pro-Glu-NH$_2$ (Figure 1A) has been

A)

Wennemers catalyst   Ugi-derived Orru catalyst

B)

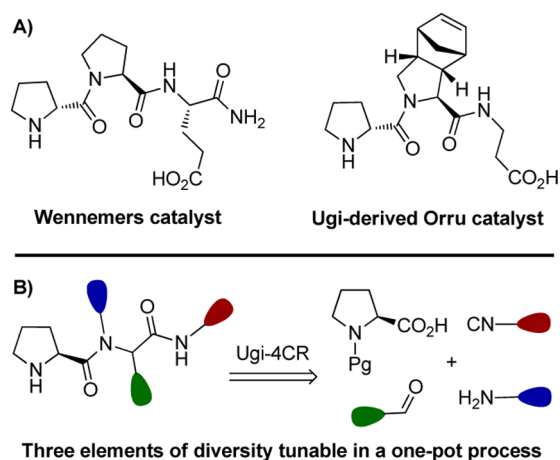Three elements of diversity tunable in a one-pot process

Figure 1. (A) Prolyl peptide catalysts for asymmetric conjugate additions. (B) Combinatorial multicomponent strategy for the preparation of prolyl peptide–peptoid hybrids.

recognized as one of the most effective catalysts for the asymmetric conjugate addition of aldehydes to nitroolefins, while other analogues have been also developed for the catalytic asymmetric Aldol reaction.[9]

Perhaps the MCR of greater promise in the field of peptide catalysis is the Ugi four-component reaction (Ugi-4CR).[10] This reaction has proven to be a powerful tool for the efficient preparation of peptidic skeletons, including N-alkylated peptides and a wide variety of peptidomimetics.[3,11] Recently, Orru and co-workers[12] implemented a highly diastereoselective Ugi reaction for the straightforward synthesis of a prolyl peptide resembling the structure and catalytic behavior of Wennemers catalyst (Figure 1A), which proved the potential of such a reaction for accessing target peptides.

Herein we report the application of the Ugi-4CR for the combinatorial development of novel peptide–peptoid hybrid catalysts as well as the assessment of their catalytic behavior in the asymmetric conjugate addition of aldehydes to nitroolefins. As depicted in Figure 1B, our strategy focuses on exploiting the diversity-generating capability of this reaction in the solution-phase production of a collection of compounds integrating structural elements of peptides and peptoids (in sensu stricto, peptoids are defined as N-substituted polyglycines). Thus, this approach differs from that of Orru and co-workers[12] in the sense that the use of the MCR does not aim at the synthesis of a target peptide catalyst but rather at a collection of them to address the effect of the structural variations on the catalytic profile.

■ RESULTS AND DISCUSSION

Solution-Phase Multicomponent Synthesis of Prolyl Peptide–Peptoid Hybrid Catalysts. The classic Ugi-4CR[10] is the one-pot condensation of a primary amine, an oxo compound (i.e., ketone or aldehyde), a carboxylic acid, and an isocyanide to produce an N-substituted dipeptide backbone, which may be considered as a peptide–peptoid hybrid[13] when an α-amino acid is used as either the carboxylic acid or amino component. As proposed early by Ugi himself, the multicomponent nature of this process enables the development of powerful combinatorial procedures through variation of each of the four starting materials. Whereas this concept has been previously applied in drug discovery,[6] we are not aware of its implementation in organocatalyst discovery.[14] As illustrated in

Figure 1B, we planned the installation of three elements of tunable diversity, namely, the amine, oxo, and isocyanide components, while retaining proline as a fixed substrate with the aim of enabling enamine catalysis. As a result, the simple variation of highly available substrates such as primary amines, carbonyl compounds, and isocyanides may give rise to a medium-sized library of structurally novel prolyl peptide–peptoid hybrids for screening of their catalytic behavior.

As shown in Table 1, the implementation of the multi-component combinatorial approach required a two-step

Table 1. Multicomponent Combinatorial Synthesis of Prolyl Peptide–Peptoid Hybrid Catalysts Using the Ugi-4CR Either at Room Temperature or under Microwave Irradiation
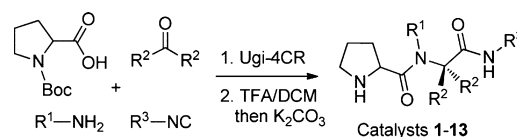
entry	acid	R^1	R^2	R^3	catalyst	yield (%)[c]
1	L-Pro	Gly-OMe[a]	H	Cy	1	78
2	L-Pro	Val-OMe[b]	H	Cy	2	81
3	L-Pro	Leu-OMe[b]	H	Cy	3	85
4	L-Pro	Ile-OMe[b]	H	Cy	4	77
5	L-Pro	Phe-OMe[b]	H	Cy	5	83
6	L-Pro	^{t}BuGly-OMe[b]	H	Cy	6	61
7	L-Pro	(S)-α-MeBn[a]	H	Cy	7	91
8	L-Pro	Bn[a]	H	Cy	8	93
9	L-Pro	(S)-α-MeBn[a]	Me	Cy	9	77
10	L-Pro	Bn[a]	Me	Cy	10	73
11	L-Pro	(S)-α-MeBn[a]	H	^{t}Bu	11	88
12	L-Pro	(S)-α-MeBn[a]	H	Gly-OMe	12	82
13	D-Pro	(S)-α-MeBn[a]	Me	Cy	13	79

[a]Reaction conducted at room temperature in MeOH for 24 h. [b]Reaction conducted under microwave irradiation. [c]Yields of isolated pure products over two steps.

procedure comprising the one-pot assembly of the peptidic skeleton by the Ugi-4CR followed by N-terminus deprotection. Among the three distinct elements of diversity, initial attention was focused on variation of the amine (entries 1–8) while paraformaldehyde and cyclohexyl isocyanide were kept as fixed components. A typical Ugi protocol[10b] was implemented for all of the catalysts in a first instance, which proved to be suitable for reactive amines (entries 1 and 7–12) but gave poor results when sterically congested α-amino acid methyl esters were used (entries 2–6).
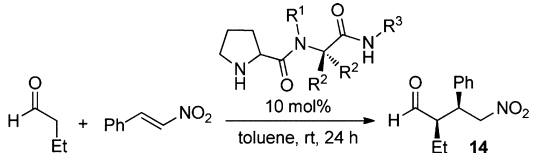
The solution for this was the use of microwave irradiation, which exhibited good efficiency in the multicomponent preparation of catalysts 2–6, whereas up to three irradiation cycles (30 min, 150 W, 70 °C) were required in the reaction of the unreactive L-tert-butylglycine methyl ester (entry 6). We next looked into the variation of the oxo and isocyano components, again relying on the use of readily available starting materials to produce accessible catalysts. Thus, acetone was utilized as the oxo component in combination with both (S)-α-methylbenzyl and benzyl amines (entries 9 and 10), leading to catalysts 9 and 10 having the sequence Pro-N-alkyl-Aib (where Aib is α-aminoisobutyric acid). Alternatively, tert-butyl isocyanide and methyl isocyanoacetate were combined

with (*S*)-α-methylbenzylamine and paraformaldehyde (entries 11 and 12) to produce catalysts **11** and **12**. In a last instance, (*S*)-α-methylbenzylamine, acetone, and cyclohexyl isocyanide were combined with D-Pro to produce catalyst **13**, an analogue of **9** having the opposite stereochemistry at proline. We envisioned that with this we might be able to assess the actual role of the pyrrolidine ring stereochemistry on the stereo-control induced by such catalysts. Alternatively, with the changes in the amino and isocyano components we aimed to address the influence on the catalytic profile of the bulky character of substituents at both the internal and *C*-terminal amides. On the other hand, the variation of *N*-alkyl-Gly to *N*-alkyl-Aib (derived from the change of formaldehyde to acetone, respectively) aimed to address the influence of the peptide conformational flexibility on the catalytic performance. It must be noticed that the utilization of prochiral aldehydes and ketones in this combinatorial protocol is certainly possible, whereas this initial study skipped the difficulty associated with the separation and identification of the resulting diastereomers.

Assessment of the Enamine-Type Catalytic Performance. With the library of peptide−peptoid hybrid catalysts in hand, we turned to the evaluation of their organocatalytic performance in the Michael addition. This class of chemical transformation is recognized as one of the most powerful C−C bond-forming reactions,[15] and since the discovery of its aminocatalytic version[16] it has been traditionally selected for assessing the potential of new catalysts acting through enamine catalysis.[1] Important insights into the mechanism of the catalytic conjugate addition of aldehydes to nitroolefins have been reported in recent years[17] with the use of the diphenylprolinol silyl ether, one of the most effective catalysts in the stereoselective version of this process.[18] To screen the performance of peptide−peptoid hybrids **1**−**12**, their catalytic efficiencies and stereoselection were initially assessed in the model system consisting of the conjugate addition of *n*-butanal to *trans*-β-nitrostyrene. During the initial screening, standard reaction conditions consisting of the use of 10 mol % catalyst in toluene as the solvent at room temperature were chosen.

As illustrated in Table 2, most of the compounds catalyzed the Michael addition with good to excellent enantio- and diastereoselectivity, with catalyst **9** showing the best results in terms of stereocontrol (98% ee, 94:6 dr). Analysis of these results provides important insights into the structural requirements (derived from the three elements of diversity) for this new class of catalysts to be effective. Thus, in terms of chemical efficiency and diastereoselection, there does not seem to be a great difference among these catalysts, whereas the enantiose-lection was found to be more dependent on some of the variable structural elements. Among these tunable structural elements, variation of the chirality and bulky character of the *N*-substituent derived from the amino component (entries 1−8) did not lead to a clear tendency in the enantioselectivity behavior when formaldehyde was employed as the oxo component. As depicted in Table 2, the presence of the achiral *N*-substituents Gly-OMe (entry 1) and benzylamine (entry 8) provided similar results (i.e., ca. 90% ee) as the chiral ones Val-OMe (entry 2), Ile-OMe (entry 4), and (*S*)-α-methylbenzyl-amine (entry 7). Alternatively, Val-OMe (entry 2) and Ile-OMe (entry 4) showed much better enantioselectivity than Leu-OMe (entry 3) and Phe-OMe (entry 5), but intriguingly, L-*t*BuGly (entry 6) gave only moderate results despite the fact that it has the bulkiest side chain among all of the amino acid methyl esters incorporated as *N*-substituents.

Table 2. Screening of the Enamine-Type Catalytic Performance of Peptide−Peptoid Hybrids 1−13 in the Asymmetric Michael Addition[a]

entry	acid/R¹/R²/R³	yield (%)[b]	dr (syn/anti)[c]	ee (%)[d]
1	L-Pro/Gly-OMe/H/Cy (**1**)	87	96:4	90
2	L-Pro/Val-OMe/H/Cy (**2**)	92	92:8	91
3	L-Pro/Leu-OMe/H/Cy (**3**)	83	97:3	79
4	L-Pro/Ile-OMe/H/Cy (**4**)	89	97:3	90
5	L-Pro/Phe-OMe/H/Cy (**5**)	84	93:7	64
6	L-Pro/*t*BuGly-OMe/H/Cy (**6**)	94	90:10	82
7	L-Pro/MeBn/H/Cy (**7**)	74	96:4	89
8	L-Pro/Bn/H/Cy (**8**)	91	93:7	92
9	L-Pro/MeBn/Me/Cy (**9**)	85	94:6	98
10	L-Pro/Bn/Me/Cy (**10**)	84	94:6	87
11	L-Pro/MeBn/H/*t*-Bu (**11**)	93	94:6	91
12	L-Pro/MeBn/H/Gly-OMe (**12**)	77	89:11	85
13	D-Pro/MeBn/Me/Cy (**13**)	93	84:16	−86

[a]All of the reactions were conducted using 3 equiv of the aldehyde. [b]Yields of isolated products as mixtures of *syn* and *anti* adducts. [c]Determined by ¹H NMR spectroscopy of the crude mixture and HPLC analysis. [d]Determined by chiral-stationary-phase HPLC analysis of the major diastereomer.

On the other hand, the incorporation of the amino acid residue Aib (derived from the use of acetone instead of formaldehyde as the oxo component) shed additional light on the structure−catalytic activity relationship. Thus, the combi-nation of Aib (R² = Me) and the chiral (*S*)-α-methylbenzyl group as the *N*-substituent led to the most effective catalyst, **9** (98% ee; Table 2, entry 9). Intriguingly, catalyst **10** bearing benzyl as the *N*-substituent exhibited only moderate enantioselectivity (entry 10), despite the fact that it also has the amino acid residue Aib (R² = Me) derived from the use of acetone in the Ugi-4CR.

We next looked at how the stereocontrol of the conjugate addition was affected by varying the isocyanide component while keeping the oxo and amino components fixed [i.e., R¹ = (*S*)-α-MeBn and R² = H]. Thus, catalyst **11** (R³ = *t*Bu, entry 11) showed a slightly higher enantioselectivity than its analogue **7** (R³ = Cy, entry 7), probably because of the bulkier character of the *tert*-butyl amide substituent compared with the cyclohexyl one. In contrast, the incorporation of the less bulky methyl isocyanoacetate in catalyst **12** (R³ = Gly-OMe, entry 12) led to a drop in both the enantio- and diastereoselectivity with respect to catalyst **7**. On the basis of these results, it can be stated that the incorporation of an isocyanide component with certain steric hindrance is important, although there are no great differences between catalysts having the terminal *tert*-butyl and cyclohexyl carboxamides. Thus, the use of cyclohexyl isocyanide becomes more feasible than *tert*-butyl isocyanide because of the lower price and simpler synthesis of the former.

Finally, catalyst **13** provided good enantio- and diaster-eoselectivity while producing the Michael adduct with the reverse configuration at the asymmetric centers (Table 2, entry 13), thus proving that the stereocontrol is mainly biased by the

pyrrolidine ring stereochemistry. Nevertheless, in this case the topological matching with the (S)-α-methylbenzyl N-substituent is less effective than for catalyst **9** based on L-Pro, as the enantioselection of the latter was significantly higher.

At this stage, we anticipated that the increased conformational rigidity provided by the incorporation of both the amino acid Aib instead of Gly (e.g., comparison of **9** with **7**) and the chiral N-substituent (S)-α-MeBn instead of Bn (e.g., comparison of **9** with **10**) is the crucial factor in the higher enantioselectivity of catalyst **9** compared with its congeners. Such a greater conformational rigidity of **9**, derived from both the geminal methyl groups and the chiral N-substituent, was confirmed by NMR analysis. Thus, duplicate sets of signals were observed in the NMR spectra of most catalysts as a result of the presence of the *cis* and *trans* isomers of the N-substituted amide bond.[19] However, the ^{1}H NMR spectrum of catalyst **9** showed a single configurational isomer in solution, thus confirming the conformational fixation effect provided by its key structural elements.

Indeed, the above findings were possible only because of the multicomponent nature of the combinatorial procedure, in which three elements of diversity could be varied in parallel while keeping proline as a fixed component. Whereas it was proven that slight structural variations may allow for fine-tuning of the enantioselectivity, we were prompted to prepare peptide−peptoid hybrid catalysts including Aib in the backbone and amino acid methyl esters as N-substituents instead of aliphatic amines. Unfortunately, the yields of such Ugi-4CRs were rather poor even with the utilization of microwave irradiation, presumably because of inefficient imine formation starting from acetone and amino acid methyl ester hydrochlorides in the presence of 1 equiv of Et₃N.

By analysis of Table 2, peptide−peptoid hybrid **9** proved to be the most effective one under the initial reaction conditions. Therefore, we next turned to an assessment of the substrate scope of the conjugate addition catalyzed by organocatalyst **9**. As depicted in Table 3, a variety of substituted *trans-β*-nitrostyrenes were utilized to afford the corresponding Michael adducts with good to excellent enantioselectivity, albeit in some cases with only moderate diastereoselectivity. Utilization either of *trans*-2-furylnitroolefin as the acceptor (entry 9) or isovaleraldehyde as the donor (entry 2) provided Michael adducts with high diastereoselectivity but only moderate enantioselectivity.

To assess the effect of the reaction conditions on the catalytic efficiency and stereocontrol of this type of catalyst, a variety of solvents, conditions, and additives were studied. As shown in Table 4, catalyst **2** was initially chosen to accomplish this study because its performance in the model system was high (entry 1) but still improvable. In this sense, catalyst **9** was not selected for this purpose because its enantioselection was already quite high and thereby difficult to improve through variation of the conditions. Thus, neither decreasing the temperature to 5 °C (entry 1) nor adding a 10 mol % loading of either benzoic acid (entry 3) or p-nitrophenol (entry 4) provoked a significant change in the reaction yield and stereoselection. In the case of p-nitrophenol as the additive, a qualitative study revealed an initial acceleration of the reaction, although the yield was not increased after 24 h. Alternatively, decreasing the catalyst loading to 5 mol % (entry 5) and 2.5 mol % (entry 6) led to an erosion in the reaction yield, although the enantio- and diastereoselectivity remained high. Changing the solvent also decreased the effectiveness of the catalyst, especially when a

Table 3. Substrate Scope of the Asymmetric Michael Addition of Aldehydes to *trans-β*-Nitrostyrenes Catalyzed by Peptide−Peptoid Hybrid 9[a]
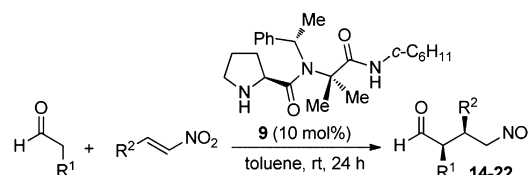
entry	R[1]	R[2]	compound	yield (%)[b]	dr (syn/anti)[c]	ee (%)[d]
1	Et	Ph	14	85	94:6	98
2	iPr	Ph	15	81	91:9	67
3	Et	4-MeOC₆H₄	16	83	82:18	93
4	Et	4-FC₆H₄	17	89	92:8	96
5	Et	4-ClC₆H₄	18	86	94:6	88
6	Et	4-BrC₆H₄	19	84	86:14	86
7	Et	2-BrC₆H₄	20	91	88:12	89
8	Et	3-NO₂C₆H₄	21	70	81:19	78
9	Et	2-furyl	22	83	93:7	82

[a]All of the reactions were conducted using 3 equiv of the aldehyde. [b]Yields of isolated products as mixtures of *syn* and *anti* adducts. [c]Determined by ^{1}H NMR spectroscopy. [d]Determined by chiral-stationary-phase HPLC analysis of the major diastereomer.

Table 4. Effect of the Reaction Conditions on the Asymmetric Michael Addition Catalyzed by Peptide−Peptoid Hybrids 2 and 3[a]
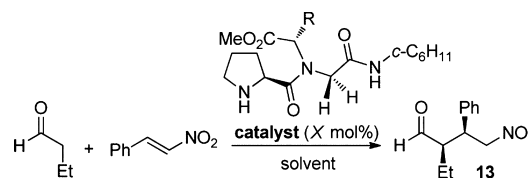
entry	catalyst	solvent	X	yield (%)[b]	dr (syn/anti)[c]	ee (%)[d]
1	2	PhMe	10	92	92:8	91
2	2	PhMe[e]	10	89	95:5	90
3	2	PhMe[f]	10	88	94:6	87
4	2	PhMe[g]	10	92	93:7	90
5	2	PhMe	5	76	94:6	89
6	2	PhMe	2.5	45	96:4	91
7	2	DCM	10	74	94:6	79
8	2	PhMe/iPrOH[h]	10	90	95:5	80
9	2	CH₃Cl/iPrOH[h]	10	63	93:7	62
10	2	iPrOH	10	98	85:15	34
11	2	THF	10	98	88:12	73
12	3	PhMe	10	83	68:32	79
13	3	PhMe[f]	10	57	94:6	49
14	3	CH₃Cl/iPrOH[h]	10	61	94:6	47
15	3	THF	10	91	90:10	64

[a]Reactions were conducted using 3 equiv of the aldehyde and, unless otherwise specified, at room temperature for 24 h. [b]Yields of isolated products as mixtures of *syn* and *anti* adducts. [c]Determined by ^{1}H NMR analysis of the crude mixture and HPLC analysis. [d]Determined by chiral-stationary-phase HPLC analysis of the major diastereomer. [e]Reaction was conducted at 5 °C. [f]10 mol % benzoic acid was used as an additive. [g]10 mol % p-nitrophenol was used as an additive. [h]Solvent mixture 9:1 (v/v).

very polar solvent was employed. Hence, either DCM or a mixture containing a small amount of iPrOH (entries 8 and 9)

were less successful than pure toluene, while both pure [i]PrOH and THF provoked an improvement in the reaction yield but a marked drop in the enantio- and diastereoselection. Whereas this proves that nonprotic, hydrophobic solvents are required for good stereocontrol, the results are quite intriguing since a $CHCl_3$/[i]PrOH mixture is the solvent of choice for Michael additions with Wennemers' peptide catalysts.[8]

As illustrated in Table 4, we also decided to evaluate catalyst **3** under a variety of conditions, considering that the effectiveness of this catalyst might be improvable. However, neither the presence of an acid additive (entry 13) nor the utilization of a more polar solvent such as $CHCl_3$/[i]PrOH (entry 14) or THF (entry 15) led to higher enantio- and diastereoselectivity compared with the original conditions (entry 12).

For catalysts derived from L-proline, the absolute configuration of the Michael adducts was unambiguously established to be 2R,3S according to chemical correlation with previous reports (see the Experimental Section). This enantioselection can be explained according to Seebach's topological model,[20] in which the *anti*-enamine approaches the nitroolefin at the less hindered face through a synclinal transition state. To understand the enantioselectivity observed in this work, the peptidic substituent at the pyrrolidine ring must favor the formation of the enamine with the *E* configuration while providing important shielding of the *Re* face. Accordingly, we were prompted to undertake a conformational study aimed at understanding both the actual shielding effect of one of the pyrrolidine (and therefore enamine) faces and the dissimilar *cis*−*trans* isomerizations detected by NMR analysis for catalysts incorporating either *N*-substituted Gly or Aib.

Conformational Analysis. A conformational analysis was accomplished for the parent catalysts **7** and **9**, keeping in mind that (*i*) the stereocontrol provided by **9** was higher that of **7** and (*ii*) NMR analysis of **9** showed almost a single configurational isomer while that of **7** showed a mixture of *cis* and *trans* isomers in solution (see the NMR spectra in part A of the Supporting Information).

To cover the conformational space of catalyst **7**, we initially conducted a conformational search by Monte Carlo molecular mechanics (MCMM) as implemented in MacroModel version 9.9. We were able to find 673 different conformers within 5 kcal mol^{-1} of the lowest-energy conformation. Clustering according to the atomic distances of heavy atoms eliminated the redundant conformers, resulting in 42 groups (see part B of the Supporting Information). The same conformational search was performed with catalyst **9** and resulted in 182 different conformers and 26 groups after clustering analysis. Representative structures of low-energy clustered conformers were selected and reoptimized at the M06-2X/6-31G(d) level. The electronic energies were refined by single-point calculations using the 6-31+G(d,p) basis set. The relative Gibbs energies and Boltzmann populations at 25 °C in CDCl$_3$ for all of the reoptimized low-energy conformers are shown in part B of the Supporting Information (see Tables S1, S2, S3, and S4).

As shown in Figure 2, analysis of the superposed geometries of these reoptimized low-energy conformers indicated that a restricted conformational space was adopted by the conformers. Nevertheless, it is evident that the conformational rigidity of catalyst **9** is higher than that of **7**, confirming the NMR behavior of both catalysts. The notation used to represent the conformations of catalysts **7** and **9** is focused on the plane through the tertiary amide bond. As can be seen in the
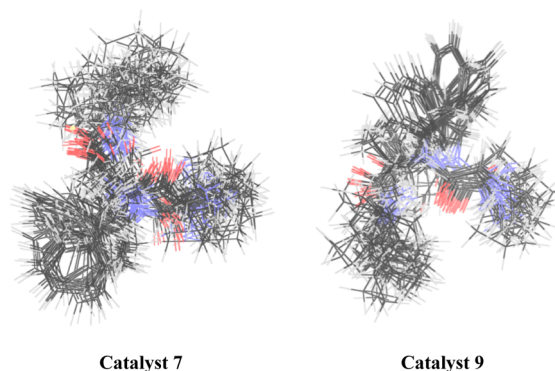

Figure 2. Superpositions of low-energy clusters of conformers of catalysts **7** and **9** calculated at the M06-2X/6-31+G(d,p)//M06-2X/6-31G(d) [SDM, chloroform] level.

graphical representation in Table 5, the Ph and *N*-cyclohexyl groups were selected to define the positive (+) and negative

Table 5. Graphical Representation and Excerpt of the Dihedral Distributions for Catalysts 7 and 9

catalyst	isomer	$\Psi_1(+)/\Psi_2(-)$	$\Psi_1(-)/\Psi_2(+)$	$\Psi_1(+)/\Psi_2(+)$	$\Psi_1(-)/\Psi_2(-)$
7 (R = H)	*cis*	0.1	39.2	2.6	0.0
	trans	42.0	0.0	0.7	15.2
9 (R = Me)	*cis*	17.3	9.9	17.3	53.6
	trans	0.0	0.0	0.0	1.9

(−) orientations of the dihedrals Ψ_1 and Ψ_2 (see in Tables S2 and S4 in part B of the Supporting Information for the assignment of each conformer in this notation). After examination of the dihedral orientations of the different conformers of catalyst **7** (Table 5), a *cis/trans* ratio of 42:58 was determined. In contrast, conformational analysis of catalyst **9** revealed an inversion in the equilibrium, with a *cis/trans* ratio of 98:2 as well as a marked difference in the orientations of the dihedrals compared with catalyst **7**.

The fact that *cis* conformers of **9** (R = Me) are lower in energy (and thus more populated) than those of catalyst **7** (R = H) seems to be a crucial factor in understanding the difference in the enantioselectivities. As depicted in Figure 2, partial shielding of one of the pyrrolidine ring faces is observed in the low-energy clustered conformers of both **7** and **9**, although this is indeed more marked in the case of catalyst **9** that is 98% populated with *cis* conformers. To further confirm these results experimentally, two NOESY spectra were recorded for catalyst **9** in CDCl$_3$ in order to determine the disposition of the peptidic chain with respect to the pyrrolidine faces (see part A of the Supporting Information). Initially, a NOESY spectrum with irradiation of the C*H* signal of the methylbenzyl *N*-substituent at 5.11 ppm showed NOE effects with one of the methylene *β*-hydrogens of proline, which proves the *cis* configuration proposed by molecular modeling. Alternatively, a second NOESY experiment was accomplished with irradiation of the N*H* signal of the cyclohexyl amide at 5.74 ppm, resulting

in NOE effects with hydrogens of the cyclohexyl ring, with the *ortho* hydrogens of the phenyl ring, with one of the *gem*-dimethyl groups of the Aib residue, and with a β-hydrogen of proline. However, the lack of an NOE with the α-hydrogen of proline at 4.30 ppm, which is positioned at the nonsubstituted pyrrolidine face, is a clear indication that the peptidic skeleton is directed toward the substituted pyrrolidine face. This fully agrees with the *cis* isomer structures of catalyst **9** shown in Figures 2, 3, and 5, wherein the terminal cyclohexyl moiety is positioned at the opposed face of the proline α-hydrogen, thus setting free the nonsubstituted face upon enamine formation and further addition to the Michael acceptor. Indeed, such a shielding effect over a specific pyrrolidine face is biased by the proline stereochemistry, and it is hypothesized to be reversed in a catalyst having the opposite configuration at the proline and methylbenzyl stereocenters.

To assess whether the blocking of one of the pyrrolidine faces remains upon enamine formation, a conformational search was performed for the *anti*-enamine derived from catalyst **9** and the aliphatic aldehyde. As shown in Figure 3, the optimized
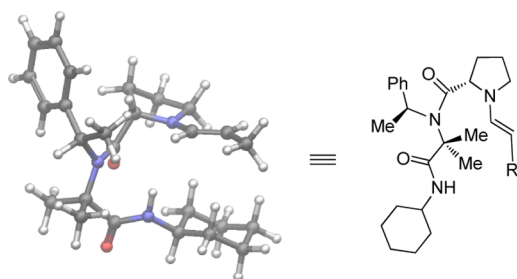

Figure 3. Lowest-energy structure of the *anti*-enamine derived from catalyst **9**.

lowest-energy structure of the enamine with *E* configuration shows a significant shielding of the peptidic skeleton to the *Re* face, which according to Seebach's topological model explains the high enantioselection provided by catalyst **9**.

As shown in Figure 4, conformational analysis of **7** shed additional light on the *cis*−*trans* isomerization. We detected

that the most populated *trans* conformers of **7** were the Ψ_1 dihedral rotamers **11**-*trans* (38%) and **36**-*trans* (13%). Another significant feature was the relative orientation of dihedrals Ψ_1 and Ψ_2. Thus, *cis* conformers of **7** adopt a $\Psi_1(-)/\Psi_2(+)$ orientation and *trans* conformers a $\Psi_1(+)/\Psi_2(-)$ orientation, with the Ph and *N*-cyclohexyl groups positioned in opposite directions. We also noticed persistent NH···O=C hydrogen bonding between the pyrrolidine σ^*_{N-H} group and the oxygen lone pairs $LP_{O(1)/O(2)}$ of the tertiary amide carbonyl group in a wide set of conformers of catalyst **7** (see section S1 in part B of the Supporting Information). In addition, we investigated the transition state **TS-1** that represents the *cis*−*trans* equilibration from the more populated **11**-*trans* conformer (31%) to the **20**-*cis* conformer (26%). The result was an activation energy of 21 kcal/mol, which explains the detection of both configurational isomers of catalyst **7** on the NMR time scale. The natural bond orbital (NBO) analysis of the selected structures **36**-*trans*, **11**-*trans*, **TS-1**, and **20**-*cis* showed delocalization energies in the range from 1.64 to 4.57 kcal mol^{-1}. The geometries, Boltzmann populations, and Gibbs energies of conformers involving the main *cis*−*trans* isomerization of catalyst **7** are also represented in Figure 4.

Interestingly, an additional stabilizing hydrogen-bonded intramolecular seven-membered ring was detected, involving the same $LP_{O(1),O(2)}$ and amide σ^*_{N-H} group (CONH···O=C) of the more hindered **20**-*cis* conformer, with energy of 6.12 kcal mol^{-1} (see part B of the Supporting Information). This explains the slightly higher stability of the lowest-energy **11**-*trans* isomer compared with **20**-*cis*. Although such hydrogen bonding may be relevant for this analysis only in the ground state of the catalyst, it must be noted that is even preserved in **TS-1**, comprising a high stabilization energy of 11.55 kcal mol^{-1}.

As depicted in Figure 5, conformational analysis of catalyst **9** revealed that **1**-*trans* (2%) and the lowest-energy conformer **26**-*cis* (33%) adopted a $\Psi_1(-)/\Psi_2(-)$ orientation directed axially (according to the imaginary plane of the tertiary amide carboxyl) to the methyl group of the (*S*)-α-MeBn *N*-substituent. This orientation is directed by steric clashes involving the equatorial *N*-alkyl H ↔ Me interaction present in **1**-*trans*, while the Me ↔ Me interaction increases the energy of
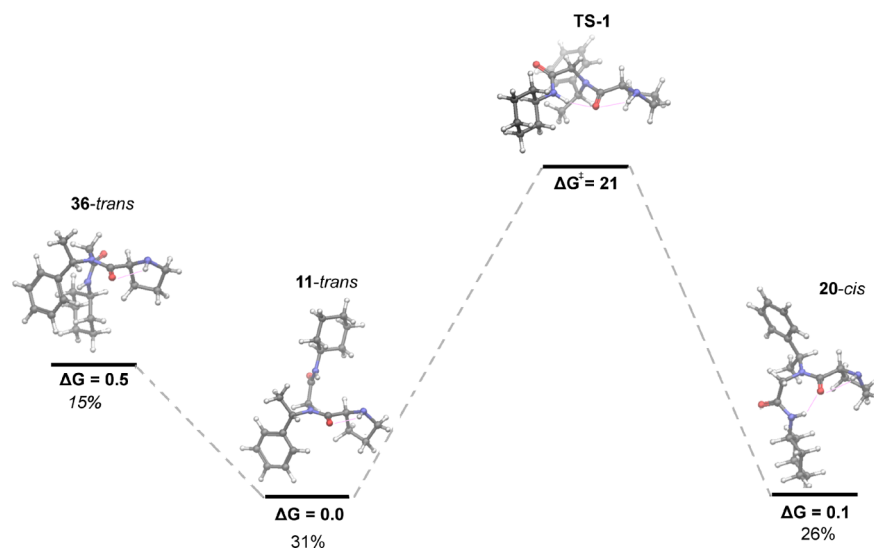

Figure 4. Relevant low Gibbs energy *cis*−*trans* conformers and transition state of catalyst **7** at the M06-2X/6-31+G(d,p)//M06-2X/6-31G(d) [SDM, chloroform] level.
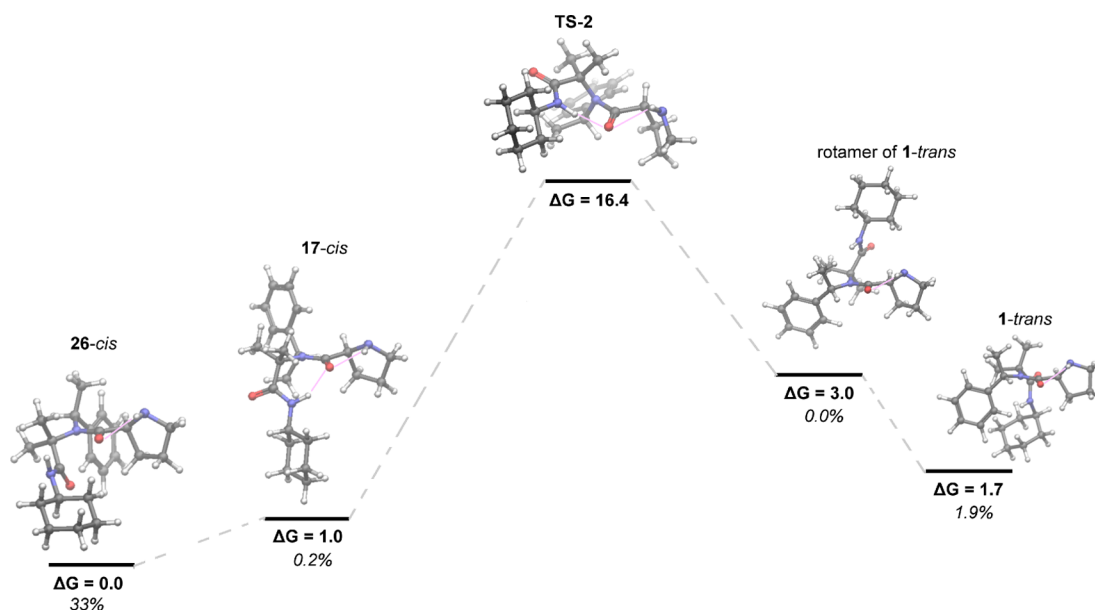
Figure 5. Relevant low Gibbs energy *cis*−*trans* amide conformers and transition state of catalyst **9** at the M06-2X/6-31+G(d,p)//M06-2X/6-31G(d) [SDM, chloroform] level.

17-*cis* (8%), a Ψ_1 dihedral rotamer of **26**-*cis* (Figure 3), by 1 kcal mol^{-1}. Similarly to catalyst **7**, persistent hydrogen bonding involving the pyrrolidine σ^*_{N-H} group (NH···O=C) was observed for **9** (see section S2 in part B of the Supporting Information). NBO analyses of **1**-*trans* and its rotamer (not located by the MM conformational search and drawn manually) as well as **17**-*cis*, **26**-*cis*, and **TS-2**, showed delocalization energies in the range of 1.68 to 4.59 kcal mol^{-1}. Interestingly, the located transition state **TS-2** comprises an activation energy of 15 kcal mol^{-1} (6 kcal mol^{-1} less than observed for catalyst **7**), which allows for a relatively fast shift of the equilibrium to the less energetic *cis* isomer.

The additional intramolecular hydrogen-bonded seven-membered ring (CONH···O=C) was absent in the lowest-energy conformer **26**-*cis* but was found in the **17**-*cis* conformer (8.26 kcal mol^{-1}) and in **TS-2** (13.76 kcal mol^{-1}) as well. Unexpectedly, **TS-2** leads to a shorter hydrogen bond than **TS-1** (1.886 and 1.952 Å, respectively), thus reflecting the crowded transition structure. The geometries, Boltzmann populations, and Gibbs energies of these representative structures are represented in Figure 5.

CONCLUSION

This study has shown that solution-phase combinatorial approaches based on isocyanide-based MCRs are convenient tools for the discovery of organocatalysts for asymmetric organic transformations. We have illustrated this by the Ugi-4CR-based generation of a small combinatorial collection of new prolyl peptide−peptoid hybrids and the screening of their catalytic efficacies in the asymmetric conjugate addition of aldehydes to nitroolefins. Thus, variation of three elements of diversity in the Ugi-derived *N*-substituted peptide led to the discovery of catalysts providing good to excellent stereocontrol and catalytic efficacy and provided new insights into their structure−catalytic activity relationship. A conformational study explained the greater conformational rigidity and stereo-selection provided by catalyst **9** bearing the *N*-substituted amino acid Aib as the C-terminal residue compared with **7** that has Gly at the same position. In view of the diversity-oriented

character of MCRs, further exploitation of this capacity in the combinatorial discovery of catalysts is foreseeable.

EXPERIMENTAL SECTION

General Experimental. Melting points are uncorrected. ^{1}H NMR and ^{13}C NMR spectra were recorded at 400 MHz for ^{1}H and 100 MHz for ^{13}C, respectively. Chemical shifts (δ) are reported in parts per million relative to tetramethylsilane (TMS), and coupling constants (J) are reported in hertz. High-resolution ESI mass spectra were obtained using a Fourier transform ion cyclotron resonance (FT-ICR) mass spectrometer, an RF-only hexapole ion guide, and an external electrospray ion source. Flash column chromatography was carried out using silica gel 60 (230−400 mesh), and analytical thin-layer chromatography (TLC) was performed using silica gel aluminum sheets. HPLC chromatograms were obtained on an apparatus with an LC-10AT pump, an SPD-10A UV−vis detector, and an SCL-10A system controller using a Chiralpak AD-H column (4.6 mm diameter × 250 mm length, particle size 5 μm). Optical rotations were measured with a polarimeter at 589 nm and 30 °C.

Syntheses. *General Ugi-4CR-Based Procedure.* A suspension of the amine (1.0 mmol) and the aldehyde or ketone (1.0 mmol) in MeOH (5 mL) was stirred for 1 h at room temperature. NEt$_3$ (1.0 mmol) was added when α-amino acid methyl ester hydrochlorides were employed. The carboxylic acid (1.0 mmol) and the isocyanide (1.0 mmol) were then added, and the reaction mixture was stirred at room temperature for 24 h. The volatiles were concentrated under reduced pressure, and the resulting crude product was dissolved in 100 mL of CH$_2$Cl$_2$. The organic phase was washed sequentially with a saturated aqueous solution of citric acid (50 mL), aqueous 10% NaHCO$_3$ (50 mL), and brine (50 mL) and then dried over anhydrous Na$_2$SO$_4$ and concentrated under reduced pressure. The resulting amorphous solid was used in the Boc deprotection step without further purification.

General Procedure for Microwave-Assisted Ugi-4CR. The amine (1.0 mmol) and the aldehyde (1.0 mmol) were dissolved in MeOH (5 mL) and added to a 10 mL glass tube. NEt$_3$ (1.0 mmol) was added when α-amino acid methyl ester hydrochlorides were employed. The suspension was treated with the carboxylic acid (1.0 mmol) and the isocyanide (1.0 mmol), and the glass tube was sealed and introduced into a CEM Discovery focused microwave oven. The flask was irradiated for 30 min (150 W) under high-speed magnetic stirring while the temperature was raised to 70 °C. The reaction course was monitored by TLC, and additional cycles of 30 min were applied in

cases of poor consumption of the starting material. The volatiles were concentrated under reduced pressure, and the resulting crude product was dissolved in 100 mL of CH_2Cl_2. The organic phase was washed sequentially with a saturated aqueous solution of citric acid (50 mL), aqueous 10% $NaHCO_3$ (2 × 50 mL), and brine (50 mL) and then dried over anhydrous Na_2SO_4 and concentrated under reduced pressure. The resulting amorphous solid was used in the Boc deprotection step without further purification.

General Procedure for Boc Deprotection. The crude product resulting from the Ugi-4CR was dissolved in 3 mL of CH_2Cl_2 and treated with 1 mL of trifluoroacetic acid at 0 °C. The reaction mixture was allowed to reach room temperature, stirred for 4 h, and then concentrated to dryness (TFA was removed completely by repetitive addition and evaporation of further CH_2Cl_2). The crude product was redissolved in 10 mL of CH_2Cl_2 and treated with solid K_2CO_3 until a basic pH was achieved, and the solution was filtered and evaporated under reduced pressure.

Peptide–Peptoid Hybrid 1. HCl·Gly-OMe (125 mg, 1 mmol), triethylamine (140 μL, 1 mmol), paraformaldehyde (30 mg, 1 mmol), Boc-L-Pro-OH (215 mg, 1 mmol), and cyclohexyl isocyanide (125 μL, 1 mmol) were reacted in MeOH (5 mL) according to the general Ugi-4CR-based procedure. The resulting Boc-protected compound was subjected to the general deprotection procedure. Flash column chromatography purification (MeOH/EtOAc 4:1) afforded peptide–peptoid hybrid **1** (254 mg, 78%) as a colorless oil. R_f = 0.25 (n-hexane/EtOAc 1:1). $[\alpha]_D^{20}$ −15.1 (c 0.62, MeOH, 25 °C). A mixture of conformers in a 6:4 ratio was observed by NMR. ^{1}H NMR (400 MHz, CDCl$_3$): δ 1.09−1.40 (m, 6H); 1.55−1.95 (m, 6H); 1.99−2.17 (m, 3H); 2.41 (m, 1H); 3.37−3.50 (m, 2H); 3.67−3.80 (m, 1H); 3.76, 3.80 (2 × s, 3H); 4.10 (d, 1H, J = 17.2 Hz); 4.15 (m, 1H); 4.31 (d, 1H, J = 17.2 Hz); 4.96 (m, 1H); 6.95, 7.48 (2 × d, 1H, J = 8.0 Hz). ^{13}C NMR (100 MHz, CDCl$_3$): δ 24.8, 24.9, 25.3, 29.0, 32.5, 46.4, 49.4, 51.7, 52.7, 53.4, 57.9, 165.9, 169.6, 170.1. HRMS (ESI-FT-ICR) m/z: 326.2072 [M + H]$^+$; calcd for $C_{16}H_{28}N_3O_4$, 326.2069.

Peptide–Peptoid Hybrid 2. HCl·Val-OMe (168 mg, 1 mmol), triethylamine (140 μL, 1 mmol), paraformaldehyde (30 mg, 1 mmol), Boc-L-Pro-OH (215 mg, 1 mmol), and cyclohexyl isocyanide (125 μL, 1 mmol) were reacted in MeOH (5 mL) according to the microwave-assisted Ugi-4CR-based procedure using two cycles of 30 min. The resulting Boc-protected compound was subjected to the general deprotection procedure. Flash column chromatography purification (MeOH/EtOAc 4:1) afforded peptide–peptoid hybrid **2** (297.7 mg, 81%) as a colorless oil. R_f = 0.45 (n-hexane/EtOAc 1:1). $[\alpha]_D^{20}$ −56.1 (c 0.56, MeOH, 25 °C). A mixture of conformers in a 7:3 ratio was observed by NMR. ^{1}H NMR (400 MHz, CDCl$_3$): δ 0.87 (d, 3H, J = 6.6 Hz); 0.98 (d, 3H, J = 6.6 Hz); 1.06−1.39 (m, 5H); 1.54−1.91 (m, 5H); 1.94−2.54 (br. m, 5H); 3.16−3.34 (m, 1H); 3.38−3.53 (m, 2H); 3.72, 3.74 (2 × s, 3H); 3.62−3.76 (m, 1H); 3.95, 4.15 (2 × d, 1H, J = 16 Hz); 4.13, 4.25 (2 × d, 1H, J = 18 Hz); 3.81, 4.46 (2 × d, 1H, J = 10.4/9.7 Hz); 4.78, 4.85 (2 × m, 1H); 6.59, 7.11 (2 × d, 1H, J = 7.8 Hz). ^{13}C NMR (100 MHz, CDCl$_3$): δ 15.8, 20.0, 21.7, 24.6, 25.5, 29.5, 30.9, 32.8, 32.9, 44.5, 48.2, 51.1, 58.8, 67.6, 163.1, 167.5, 168.2. HRMS (ESI-FT-ICR) m/z: 368.2543 [M + H]$^+$; calcd for $C_{19}H_{34}N_3O_4$, 368.2538.

Peptide–Peptoid Hybrid 3. HCl·Leu-OMe (182 mg, 1 mmol), triethylamine (140 μL, 1 mmol), paraformaldehyde (30 mg, 1 mmol), Boc-L-Pro-OH (215 mg, 1 mmol), and cyclohexyl isocyanide (125 μL, 1 mmol) were reacted in MeOH (5 mL) according to the microwave-assisted Ugi-4CR-based procedure using two cycles of 30 min. The resulting Boc-protected compound was subjected to the general deprotection procedure. Flash column chromatography purification (MeOH/EtOAc 4:1) afforded peptide–peptoid hybrid **3** (324 mg, 85%) as a colorless oil. R_f = 0.50 (n-hexane/EtOAc 1:1). $[\alpha]_D^{20}$ −42.7 (c 0.66, MeOH, 25 °C). A mixture of conformers in a 7:3 ratio was observed by NMR. ^{1}H NMR (400 MHz, CDCl$_3$): δ 0.84−1.00 (m, 6H); 1.07−1.39 (m, 5H); 1.54−1.91 (m, 7H); 1.98−2.23 (m, 2H); 2.44 (m, 1H); 3.05 (br. s, 1H); 3.40−3.50 (m, 2H); 3.64−3.71 (m, 2H); 3.74 (s, 3H); 4.04 (d, 1H, J = 18.2 Hz); 4.19 (d, 1H, J = 18.2 Hz); 4.32 (2 × d, 1H, J = 8.8/5.1 Hz); 4.66 (t, 1H, J = 7.1 Hz); 4.79 (t, 1H, J = 7.1 Hz); 6.59, 7.56 (2 × d, 1H, J = 7.7 Hz). ^{13}C NMR (100

MHz, CDCl$_3$): δ 22.1, 22.4, 24.6, 24.9, 25.0, 25.3, 29.1, 32.3, 37.6, 38.4, 46.2, 49.2, 49.4, 52.7, 58.1, 58.3, 166.5, 170.4, 172.2. HRMS (ESI-FT-ICR) m/z: 382.2700 [M + H]$^+$; calcd for $C_{20}H_{36}N_3O_4$, 382.2698.

Peptide–Peptoid Hybrid 4. HCl·Ile-OMe (182 mg, 1 mmol), triethylamine (140 μL, 1 mmol), paraformaldehyde (30 mg, 1 mmol), Boc-L-Pro-OH (215 mg, 1 mmol), and cyclohexyl isocyanide (125 μL, 1 mmol) were reacted in MeOH (5 mL) according to the microwave-assisted Ugi-4CR-based procedure using two cycles of 30 min. The resulting Boc-protected compound was subjected to the general deprotection procedure. Flash column chromatography purification (MeOH/EtOAc 4:1) afforded peptide–peptoid hybrid **4** (294 mg, 77%) as a colorless oil. R_f = 0.50 (n-hexane/EtOAc 1:1). $[\alpha]_D^{20}$ −59.1 (c 0.65, MeOH, 25 °C). A mixture of conformers in a 1:1 ratio was observed by NMR. ^{1}H NMR (400 MHz, CDCl$_3$): δ 0.86 (t, 3H, J = 7.35 Hz); 0.94 (d, 3H, J = 6.5 Hz); 1.01−1.44 (m, 6H); 1.49−2.26 (m, 10H); 2.40, 2.49 (2 × m, 1H); 3.46 (m, 2H); 3.63−3.71 (m, 1H); 3.73 (s, 3H); 4.02, 4.16 (2 × d, 1H, J = 16.0 Hz); 4.14, 4.26 (2 × d, 1H, J = 18.2 Hz); 3.88, 4.66 (2 × d, 1H, J = 10.0 Hz); 4.81, 4.90 (2 × t, 1H, J = 8.0 Hz); 6.46, 6.85 (2 × d, 1H, J = 8.0 Hz). ^{13}C NMR (100 MHz, CDCl$_3$): δ 11.4, 15.7, 24.8, 25.2, 25.3, 25.6, 29.5, 32.4, 34.1, 46.3, 46.6, 47.00, 47.8, 48.9, 52.6, 58.4, 63.1, 166.6, 169.4, 170.9. HRMS (ESI-FT-ICR) m/z: 382.2700 [M + H]$^+$; calcd for $C_{20}H_{36}N_3O_4$, 382.2695.

Peptide–Peptoid Hybrid 5. HCl·Phe-OMe (216 mg, 1 mmol), triethylamine (140 μL, 1 mmol), paraformaldehyde (30 mg, 1 mmol), Boc-L-Pro-OH (215 mg, 1 mmol), and cyclohexyl isocyanide (125 μL, 1 mmol) were reacted in MeOH (5 mL) according to the microwave-assisted Ugi-4CR-based procedure using two cycles of 30 min. The resulting Boc-protected pseudo-peptide was subjected to the general deprotection procedure. Flash column chromatography purification (MeOH/EtOAc 4:1) afforded peptide–peptoid hybrid **5** (345 mg, 83%) as a light-yellow oil. R_f = 0.35 (n-hexane/EtOAc 1:1). $[\alpha]_D^{20}$ −87.6 (c 0.47, MeOH, 25 °C). A mixture of conformers in a 7:3 ratio was observed by NMR. ^{1}H NMR (400 MHz, CDCl$_3$): δ 1.06−1.43 (m, 5H); 1.52−1.99 (m, 5H); 2.08 (m, 2H); 2.30 (m, 1H); 3.22−3.54 (m, 4H); 3.66 (m, 1H); 3.77 (s, 3H); 4.20 (m, 1H); 4.25 (dd, 1H, J = 10.0/5.9 Hz); 4.55 (dd, 1H, J = 7.2 Hz); 7.12−7.14 (m, 1H); 7.18−7.38 (m, 4H); 7.71 (d, 1H, J = 7.8 Hz). ^{13}C NMR (100 MHz, CDCl$_3$): δ 24.7, 24.9, 25.0, 25.3, 29.1, 32.4, 34.4, 46.1, 49.2, 52.6, 53.0, 57.9, 63.8, 127.5, 128.4, 129.0, 129.2, 129.9, 136.2, 165.4, 169.5, 170.4. HRMS (ESI-FT-ICR) m/z: 416.2541 [M + H]$^+$; calcd for $C_{23}H_{34}N_3O_4$, 416.2535.

Peptide–Peptoid Hybrid 6. HCl·^{t}BuGly-OMe (182 mg, 1 mmol), triethylamine (140 μL, 1 mmol), paraformaldehyde (30 mg, 1 mmol), Boc-L-Pro-OH (215 mg, 1 mmol), and cyclohexyl isocyanide (125 μL, 1 mmol) were reacted in MeOH (5 mL) according to the microwave-assisted Ugi-4CR-based procedure using three cycles of 30 min. The resulting Boc-protected compound was subjected to the general deprotection procedure. Flash column chromatography purification (MeOH/EtOAc 4:1) afforded peptide–peptoid hybrid **6** (233 mg, 61%) as a colorless oil. R_f = 0.55 (n-hexane/EtOAc 1:1). $[\alpha]_D^{20}$ −5.9 (c 0.43, MeOH, 25 °C). A mixture of conformers in a 1:1 ratio was observed by NMR. ^{1}H NMR (400 MHz, CDCl$_3$): δ 1.05, 1.09 (2 × s, 9H); 1.00−1.43 (m, 3H); 1.55−2.02 (m, 13H); 2.19 (m, 1H); 2.50 (m, 1H); 2.81 (m, 1H); 3.13 (m, 1H); 3.55−3.65 (m, 1H); 3.73, 3.80 (2 × s, 3H); 3.67−3.77 (m, 1H); 4.12 (dd, 1H, J = 7.7/3.1 Hz); 4.18, 4.29 (2 × d, 1H, J = 18.4 Hz); 5.12 (s, 1H). ^{13}C NMR (100 MHz, CDCl$_3$): δ 23.2, 25.1, 25.4, 25.6, 27.8, 28.1, 28.6, 30.8, 32.8, 36.4, 45.6, 47.8, 50.7, 51.8, 59.2, 62.0, 164.3, 169.6, 170.0. HRMS (ESI-FT-ICR) m/z: 382.2700 [M + H]$^+$; calcd for $C_{20}H_{36}N_3O_4$, 382.2695.

Peptide–Peptoid Hybrid 7. (S)-α-Methylbenzylamine (128 μL, 1 mmol), paraformaldehyde (30 mg, 1 mmol), Boc-L-Pro-OH (215 mg, 1 mmol), and cyclohexyl isocyanide (125 μL, 1 mmol) were reacted in MeOH (5 mL) according to the general Ugi-4CR-based procedure. The resulting Boc-protected compound was subjected to the general deprotection procedure. Flash column chromatography purification (MeOH/EtOAc 4:1) afforded peptide–peptoid hybrid **7** (325 mg, 91%) as a colorless oil. R_f = 0.55 (n-hexane/EtOAc 1:1). $[\alpha]_D^{20}$ −62.8 (c 0.64, MeOH, 25 °C). A mixture of conformers in a 6:4 ratio was observed by NMR. ^{1}H NMR (400 MHz, CDCl$_3$): δ 1.01−1.36 (m,

5H); 1.49, 169 (2 × d, 3H, J = 7.2 Hz); 1.47−1.84 (m, 4H); 2.17 (m, 2H); 3.40, 2.54 (2 × m, 1H); 2.85 (br. m, 1H); 3.45 (m, 2H); 3.61 (m, 1H); 3.71, 3.89 (2 × d, 1H, J = 18.0 Hz); 3.51, 3.93 (2 × d, 1H, J = 16.0 Hz); 4.70, 5.10 (2 × m, 1H); 5.87, 6.35 (2 × q, 1H, J = 7.25 Hz); 7.22−7.40 (m, 5H); 7.72 (br. s, 1H). ^{13}C NMR (100 MHz, CDCl$_3$): δ 17.4; 24.9, 25.3, 29.8, 32.2, 32.5, 46.1, 46.6, 48.7, 49.2, 55.6, 58.2, 60.4, 127.1, 127.4, 128.6, 128.8, 129.1, 137.7, 162.7, 166.5. HRMS (ESI-FT-ICR) m/z: 358.2489 [M + H]$^+$; calcd for C$_{21}$H$_{32}$N$_3$O$_2$, 358.2483.

Peptide−Peptoid Hybrid 8. Benzylamine (110 μL, 1 mmol), paraformaldehyde (30 mg, 1 mmol), Boc-L-Pro-OH (215 mg, 1 mmol), and cyclohexyl isocyanide (125 μL, 1 mmol) were reacted in MeOH (5 mL) according to the general Ugi-4CR-based procedure. The resulting Boc-protected compound was subjected to the general deprotection procedure. Flash column chromatography purification (MeOH/EtOAc 4:1) afforded peptide−peptoid hybrid 8 (639 mg, 93%) as a pale-green oil. R_f = 0.35 (*n*-hexane/EtOAc 1:1). $[\alpha]_D^{20}$ −21.1 (*c* 0.41, MeOH, 25 °C). A mixture of conformers in a 7:3 ratio was observed by NMR. ^{1}H NMR (400 MHz, CDCl$_3$): δ 1.05−1.37 (m, 5H); 1.52−1.85 (m, 4H); 1.96−2.10 (m, 3H); 2.23, 2.38 (2 × m, 1H); 2.83 (br. s, 1H); 3.39−3.55 (m, 2H); 3.69 (m, 1H); 3.97 (m, 2H); 4.66 (m, 2H); 4.79, 4.90 (2 × m, 1H); 6.76 (d, 1H, J = 8.0 Hz); 7.18−7.40 (m, 5H). ^{13}C NMR (100 MHz, CDCl$_3$): δ 24.8, 25.0, 25.4, 29.5, 32.5, 45.9, 48.8, 49.3, 50.8, 52.2, 58.3, 127.3, 128.3, 128.5, 128.9, 129.3, 134.2, 166.4, 170.0. HRMS (ESI-FT-ICR) m/z: 344.2331 [M + H]$^+$; calcd for C$_{20}$H$_{30}$N$_3$O$_2$, 344.2328.

Peptide−Peptoid Hybrid 9. (S)-α-Methylbenzylamine (128 μL, 1 mmol), acetone (74 μL, 1 mmol), Boc-L-Pro-OH (215 mg, 1 mmol), and cyclohexyl isocyanide (125 μL, 1 mmol) were reacted in MeOH (5 mL) according to the general Ugi-4CR-based procedure. The resulting Boc-protected compound was subjected to the general deprotection procedure. Flash column chromatography purification (MeOH/EtOAc 4:1) afforded peptide−peptoid hybrid 9 (309 mg, 77%) as a colorless oil. R_f = 0.35 (*n*-hexane/EtOAc 1:1). $[\alpha]_D^{20}$ −1.9 (*c* 0.38, MeOH, 25 °C). ^{1}H NMR (600 MHz, CDCl$_3$): δ 1.17−1.23 (m, 4H, CH$_2$); 1.27−1.37 (m, 2H, CH$_2$); 1.41−1.46 (m, 2H, CH$_2$); 1.48 (s, 3H, CH$_3$); 1.55 (m, 3H, CH$_3$); 1.66−1.92 (m, 4H, CH$_2$); 1.87 (d, 3H, J = 7.0 Hz, CH$_3$); 2.13 (m, 1H, CH$_2$); 2.33 (m, 1H, CH$_2$); 3.24 (m, 2H, CH$_2$); 3.37 (m, 1H, CH$_2$); 3.60 (m, 1H, CH); 4.30 (m, 1H, CH); 5.11 (m, 1H, CH); 5.74 (d, 1H, J = 7.3 Hz, NH); 7.24 (t, 1H, J = 7.5 Hz, CH); 7.36 (t, 2H, J = 7.6 Hz, CH); 7.57 (d, 2H, J = 7.7 Hz, CH). ^{13}C NMR (150 MHz, CDCl$_3$): δ 19.2 (CH$_3$), 24.3, 24.7, 24.9, 25.0, 25.5 (CH$_2$), 27.8, 28.4 (CH$_3$), 28.9, 32.7, 46.3 (CH$_2$), 48.9, 51.8, 59.7 (CH), 64.9 (C), 127.3, 128.0, 129.2 (CH), 140.8 (C), 170.8, 173.4 (C=O). HRMS (ESI-FT-ICR) m/z: 386.2800 [M + H]$^+$; calcd for C$_{23}$H$_{36}$N$_3$O$_2$, 386.2802.

Peptide−Peptoid Hybrid 10. Benzylamine (110 μL, 1 mmol), acetone (74 μL, 1 mmol), Boc-L-Pro-OH (215 mg, 1 mmol), and cyclohexyl isocyanide (125 μL, 1 mmol) were reacted in MeOH (5 mL) according to the general Ugi-4CR-based procedure. The resulting Boc-protected compound was subjected to the general deprotection procedure. Flash column chromatography purification (MeOH/EtOAc 4:1) afforded peptide−peptoid hybrid 10 (229 mg, 73%) as a colorless oil. R_f = 0.35 (*n*-hexane/EtOAc 1:1). $[\alpha]_D^{20}$ −20.6 (*c* 0.41, MeOH, 25 °C). ^{1}H NMR (400 MHz, CDCl$_3$): δ 1.06−1.39 (m, 5H); 1.46 (s, 3H); 1.50 (s, 3H); 1.55−1.75 (m, 3H); 1.78−2.06 (m, 6H); 3.03 (br. m, 1H); 3.40 (m, 2H); 3.68 (m, 1H); 4.69 (m, 1H); 4.76 (d, 2H, J = 6.91 Hz); 5.98 (d, 1H, J = 8.0 Hz); 7.22−7.44 (m, 5H). ^{13}C NMR (100 MHz, CDCl$_3$): δ 24.1, 24.5, 24.9, 25.4, 29.7, 32.6, 32.7, 46.0, 47.9, 48.8, 58.9, 64.1, 126.4, 128.0, 129.2, 136.9, 169.9, 173.0. HRMS (ESI-FT-ICR) m/z: 372.2651 [M + H]$^+$; calcd for C$_{22}$H$_{33}$N$_3$O$_2$, 372.2654.

Peptide−Peptoid Hybrid 11. (S)-α-Methylbenzylamine (128 μL, 1 mmol), paraformaldehyde (30 mg, 1 mmol), Boc-L-Pro-OH (215 mg, 1 mmol), and *tert*-butyl isocyanide (125 μL, 1 mmol) were reacted in MeOH (5 mL) according to the general Ugi-4CR-based procedure. The resulting Boc-protected compound was subjected to the general deprotection procedure. Flash column chromatography purification (MeOH/EtOAc 4:1) afforded peptide−peptoid hybrid 11 (298 mg, 88%) as a light-yellow oil. R_f = 0.55 (*n*-hexane/EtOAc 1:1). $[\alpha]_D^{20}$ −78.9 (*c* 0.65, MeOH, 25 °C). A mixture of conformers in a 8:2 ratio

was observed by NMR. ^{1}H NMR (400 MHz, CDCl$_3$): δ 1.23, (2 × s, 6H); 1.49 (2 × s, 3H); 1.46, 1.68 (2 × d, 3H, J = 6.88 Hz); 1.87−2.25 (m, 3H); 2.42, 2.58 (2 × m, 1H); 3.32−3.55 (m, 1H); 3.61, 3.88 (2 × d, 1H, J = 18.0 Hz); 3.45, 3.95 (2 × d, 1H, J = 16.0 Hz); 4.98, 5.11 (2 × m, 1H); 5.78 (m, 1H); 7.24−7.39 (m, 5H); 7.80 (br. s, 1H). ^{13}C NMR (100 MHz, CDCl$_3$): δ 17.4, 24.9, 28.4, 28.5, 29.9, 46.9, 47.0, 51.3, 53.6, 55.5, 58.2, 125.8, 127.0, 128.6, 128.8, 129.2, 137.9, 167.2, 170.2. HRMS (ESI-FT-ICR) m/z: 332.2330 [M + Na]$^+$; calcd for C$_{19}$H$_{30}$N$_3$O$_2$: 332.2327.

Peptide−Peptoid Hybrid 12. (S)-α-Methylbenzylamine (128 μL, 1 mmol), paraformaldehyde (30 mg, 1 mmol), Boc-L-Pro-OH (215 mg, 1 mmol), and methyl isocyanoacetate (91 μL, 1 mmol) were reacted in MeOH (5 mL) according to the general Ugi-4CR-based procedure. The resulting Boc-protected compound was subjected to the general deprotection procedure. Flash column chromatography purification (MeOH/EtOAc 4:1) afforded peptide−peptoid hybrid 12 (590.6 mg, 82%) as a light-yellow oil. R_f = 0.45 (*n*-hexane/EtOAc 1:1). $[\alpha]_D^{20}$ −18.9 (*c* 0.65, MeOH, 25 °C). A mixture of conformers in a 7:3 ratio was observed by NMR. ^{1}H NMR (400 MHz, CDCl$_3$): δ 1.55, 1.71 (2 × d, 3H, J = 6.8 Hz); 2.17 (m, 3H); 2.51 (m, 4H); 3.37−3.55 (m, 2H); 3.65, 3.70 (2 × s, 3H); 3.62, 3.81 (2 × d, 1H, J = 18.0 Hz); 3.55, 4.02 (2 × d, 1H, J = 16.2 Hz); 4.69, 4.98 (2 × m, 1H); 5.08, 5.95 (2 × m, 1H); 7.22−7.36 (m, 5H); 8.35 (m, 1H). ^{13}C NMR (100 MHz, CDCl$_3$): δ 17.4, 24.6, 29.1, 40.8, 45.6, 46.3, 52.2, 52.3, 55.6, 58.8, 127.0, 127.1, 128.6, 128.9, 129.0, 137.6, 168.8, 171.1. HRMS (ESI-FT-ICR) m/z: 348.1917 [M + H]$^+$; calcd for C$_{18}$H$_{25}$N$_3$O$_4$, 348.1915.

Peptide−Peptoid Hybrid 13. (S)-α-Methylbenzylamine (128 μL, 1 mmol), acetone (74 μL, 1 mmol), Boc-D-Pro-OH (215 mg, 1 mmol), and cyclohexyl isocyanide (125 μL, 1 mmol) were reacted in MeOH (5 mL) according to the general Ugi-4CR-based procedure. The resulting Boc-protected compound was subjected to the general deprotection procedure. Flash column chromatography purification (MeOH/EtOAc 4:1) afforded peptide−peptoid hybrid 13 (317 mg, 77%) as a colorless oil. R_f = 0.36 (*n*-hexane/EtOAc 1:1). $[\alpha]_D^{20}$ +15.6 (*c* 0.44, MeOH, 25 °C). ^{1}H NMR (400 MHz, CDCl$_3$): δ 1.07−1.41 (m, 8H); 1.54 (s, 3H); 1.57 (s, 3H); 1.61 (m, 2H); 1.67−1.83 (m 2H); 1.87 (d, 3H, J = 7.2 Hz); 1.89−2.00 (m, 3H); 2.71 (m, 1H); 3.09 (m, 2H); 3.70 (m, 2H); 5.17 (m, 1H); 5.58 (d, 1H, J = 6.3 Hz); 7.28−7.27−7.41 (m, 3H); 7.49 (d, 2H, J = 8.0 Hz). ^{13}C NMR (100 MHz, CDCl$_3$): δ 20.8, 25.2, 24.9, 25.6, 26.5, 28.5, 31.4, 32.9, 47.5, 48.4, 60.0, 64.4, 126.0, 127.2, 128.8, 142.2, 170.4, 173.9. HRMS (ESI-FT-ICR) m/z: 386.2807 [M + H]$^+$; calcd for C$_{23}$H$_{36}$N$_3$O$_2$, 386.2802.

General Procedure for the 1,4-Addition of Aldehydes to Nitroolefins (Michael Reaction). The nitroolefin (0.25 mmol, 1.0 equiv) and the aldehyde (0.75 mmol, 3.0 equiv) were added to a solution of the pseudo-peptide (0.025 mmol, 0.01 equiv) in the solvent of choice (1 mL). The reaction mixture was stirred for 24 h and then concentrated under reduced pressure. The resulting crude product was purified by flash column chromatography on silica gel using *n*-hexane/EtOAc as the eluent. The enantiomeric excess was determined by chiral-stationary-phase HPLC analysis through comparison with the authentic racemic material. Assignment of the stereoisomers was performed by comparison with literature data.

(2R,3S)-2-Ethyl-4-nitro-3-phenylbutanal (14). Prepared by the reaction of *n*-butanal with *trans*-β-nitrostyrene according to the general 1,4-addition procedure. The compound was purified by flash column chromatography (*n*-hexane/EtOAc 9:1 v/v). The spectroscopic data are in agreement with the published data.[16b] The enantiomeric excess was determined by chiral-stationary-phase HPLC (Chiralpak AD-H, *n*-hexane/^{i}PrOH 99:1, 25 °C) at 0.75 mL/min, UV detection at 210 nm: t_R = 24.6 min (syn, major), 29.3 min (syn, minor).

(2R,3S)-2-Isopropyl-4-nitro-3-phenylbutanal (15). Prepared from isovaleraldehyde and *trans*-β-nitrostyrene according to the general 1,4-addition procedure. The compound was purified by flash column chromatography (*n*-hexane/EtOAc 9:1 v/v). The spectroscopic data are in agreement with the published data.[16b] The enantiomeric excess was determined by HPLC (Chiralpak AD-H, *n*-hexane/^{i}PrOH 97:3, 25 °C) at 0.4 mL/min, UV detection at 210 nm: t_R = 24.5 min (syn, major), 28.9 min (syn, minor).

(2R,3S)-2-Ethyl-4-nitro-3-(4-methoxyphenyl)butanal **(16)**. Prepared from *n*-butanal and 1-methoxy-4-(2-nitrovinyl)benzene according to the general procedure. The spectroscopic data are in agreement with the published data.[21] The enantiomeric excess was determined by chiral-stationary-phase HPLC (Chiralpak AD-H, *n*-hexane/*i*PrOH 95:5, 25 °C) at 0.8 mL/min, UV detection at 210 nm: t_R = 16.9 min (*syn*, major), 20.8 min (*syn*, minor).

(2R,3S)-3-(4-Fluorophenyl)-2-ethyl-4-nitrobutanal **(17)**. Prepared from *n*-butanal and *trans*-4-fluoro-*β*-nitrostyrene according to the general 1,4-addition procedure. The compound was purified by flash column chromatography (*n*-hexane/EtOAc 9:1 v/v). The spectroscopic data are in agreement with the published data.[8a] The enantiomeric excess was determined by HPLC (Chiralpak AD-H, *n*-hexane/*i*PrOH 95:5, 25 °C) at 0.8 mL/min, UV detection at 210 nm: t_R = 15.4 min (*syn*, major), 19.3 min (*syn*, minor).

(2R,3S)-3-(4-Chlorophenyl)-2-ethyl-4-nitrobutanal **(18)**. Prepared from *n*-butanal and *trans*-4-chloro-*β*-nitrostyrene according to the general 1,4-addition procedure. The compound was purified by flash column chromatography (*n*-hexane/EtOAc 9:1 v/v). The spectroscopic data are in agreement with the published data.[8a] The enantiomeric excess was determined by HPLC (Chiralpak AD-H, *n*-hexane/*i*PrOH 95:5, 25 °C) at 0.8 mL/min, UV detection at 210 nm: t_R = 15.4 min (*syn*, major), 19.3 min (*syn*, minor).

(2R,3S)-3-(4-Bromophenyl)-2-ethyl-4-nitrobutanal **(19)**. Prepared from *n*-butanal and *trans*-4-bromo-*β*-nitrostyrene according to the general 1,4-addition procedure. The compound was purified by flash column chromatography (*n*-hexane/EtOAc 9:1 v/v). The spectroscopic data are in agreement with the published data.[8a] The enantiomeric excess was determined by HPLC (Chiralpak AD-H, *n*-hexane/*i*PrOH 95:5, 25 °C) at 0.8 mL/min, UV detection at 210 nm: t_R = 15.4 min (*syn*, major), 19.3 min (*syn*, minor).

(2R,3S)-3-(2-Bromophenyl)-2-ethyl-4-nitrobutanal **(20)**. Prepared from *n*-butanal and *trans*-2-bromo-*β*-nitrostyrene according to the general 1,4-addition procedure. The compound was purified by flash column chromatography (*n*-hexane/EtOAc 9:1 v/v). The spectroscopic data are in agreement with the published data.[8a] The enantiomeric excess was determined by HPLC (Chiralpak AD-H, *n*-hexane/*i*PrOH 97:3, 25 °C) at 0.5 mL/min, UV detection at 210 nm: t_R = 20.8 min (*syn*, major), 23.1 min (*syn*, minor).

(2R,3S)-2-Ethyl-4-nitro-3-(3-nitrophenyl)butanal **(21)**. Prepared from *n*-butanal and 1-nitro-3-(2-nitrovinyl)benzene according to the general 1,4-addition procedure. The compound was purified by flash column chromatography (*n*-hexane/EtOAc 9:1 v/v). The spectroscopic data are in agreement with the published data.[22] The enantiomeric excess was determined by HPLC (Chiralpak AD-H, *n*-hexane/*i*PrOH 95:5, 25 °C) at 0.8 mL/min, UV detection at 210 nm: t_R = 36.0 min (*syn*, major), 39.1 min (*syn*, minor).

(2R,3S)-2-Ethyl-4-nitro-3-(2-furyl)butanal **(22)**. Prepared from *n*-butanal and *trans*-2-(2-nitrovinyl)furan according to the general 1,4-addition procedure. The compound was purified by flash column chromatography (*n*-hexane/EtOAc 9:1 v/v). The spectroscopic data are in agreement with the published data.[22] The enantiomeric excess was determined by HPLC (Chiralpak AD-H, *n*-hexane/*i*PrOH 97:3, 25 °C) at 0.5 mL/min, UV detection at 210 nm: t_R = 22.1 min (*syn*, major), 23.9 min (*syn*, minor).

Computational Methods. The conformational searches were done in the gas phase using the Monte Carlo molecular mechanics (MCMM) method. The energy minimization was carried out using the Polak−Ribière conjugate gradient (PRCG) method[23] and the MMFF force field[24] with dielectric-constant-dependent electrostatics (e = 1) and normal cutoff points to model the nonbonded interactions, as implemented in MacroModel version 9.9.[25] All heavy atoms and hydrogens at heteroatoms were included in the test for redundant conformers using the default cutoff (maximum atom deviation) of 0.5 Å. All rotatable single bonds were included in the conformational search, even the N−C=O amide single bond. The energy window for saving new structures was 5 kcal/mol relative to the current global minimum, and a maximum number of steps of 30000 and 1000 steps per rotable bond were employed. Each search was continued until the

global energy minima were found at least 10−20 times, thus giving confidence that all of the relevant conformers had been found.

The cluster analyses were performed using a Python script, "Clustering of Conformers", interfaced to Maestro version 9.3[26] and available at the Schrödinger script center Web site.[27] Several works have shown cluster analyses in the precise description of organic molecules in solution.[28] To generate the RMS matrix, all heavy atoms and hydrogens at heteroatoms were included. The *average* method was used to calculate the best number of clusters in all cases. The low-energy structures of each cluster were selected and submitted to a full geometry optimization using quantum-mechanical methods. All of the conformers were clustered and are graphically represented in part B of the Supporting Information.

The representative (low-energy) structures of each cluster were fully optimized using the Truhlar M06-2X[29] density functional in conjunction with the 6-31G(d) basis set as implemented in Gaussian 09.[30] The SMD model[31] was used to include solvent effects for all optimizations. All Cartesian coordinates are supplied in the Supporting Information. Frequency calculations at 295.15 K (1 atm) ensured that the stationary points represented either minima (no imaginary frequencies) or transition states (a single imaginary frequency) on the potential energy surface and also furnished the zero-point vibrational energies and the thermal and entropic corrections, from which the Gibbs free energies were determined. The corresponding eigenvectors were inspected to confirm the expected isomerization transition state. The electronic energies were further refined using the 6-31+g(d,p) basis set. The natural bond orbital (NBO) analysis was calculated at the M06-2X/6-31+G(d,p) level using NBO 5.0 as implemented in Gaussian 09.

■ ASSOCIATED CONTENT

Ⓢ Supporting Information

^{1}H and ^{13}C NMR spectra of peptide−peptoid hybrid catalysts, chiral-stationary-phase HPLC analysis of Michael adducts, and complete computational data and geometries of reoptimized low-energy conformers. This material is available free of charge via the Internet at http://pubs.acs.org.

■ AUTHOR INFORMATION

Corresponding Authors
*E-mail: dgr@fq.uh.cu.
*E-mail: mwpaixao@ufscar.br. Tel. and Fax: +55-16-33518075.
Notes
The authors declare no competing financial interest.

■ ACKNOWLEDGMENTS

■ REFERENCES

(1) (a) Notz, W.; Tanaka, F.; Barbas, C. F., III. *Acc. Chem. Res.* **2004**, *37*, 580−591. (b) Grondal, C.; Jeanty, M.; Enders, D. *Nat. Chem.* **2010**, *2*, 167−178. (c) Enders, D.; Grondal, C.; Hüttl, M. R. M. *Angew. Chem., Int. Ed.* **2007**, *46*, 1570−1581. (d) Beeson, T. D.; Mastracchio, A.; Hong, J.-B.; Ashton, K.; MacMillan, D. W. C. *Science* **2007**, *316*, 582−585. (e) Mukherjee, S.; Yang, J. W.; Hoffmann, S.; List, B. *Chem. Rev.* **2007**, *107*, 5471−5569. (f) Doyle, A. G.; Jacobsen, E. N. *Chem. Rev.* **2007**, *107*, 5713−5743. (g) Melchiorre, P.; Marigo, M.; Carlone, A.; Bartoli, G. *Angew. Chem., Int. Ed.* **2008**, *47*, 6138−6171. (h) Bertelsen, S.; Jørgensen, K. A. *Chem. Soc. Rev.* **2009**, *38*, 2178−2189. (i) Tan, B.; Candeias, N. R.; Barbas, C. F., III. *Nat. Chem.* **2011**,

3, 473−477. (j) Jensen, K. L.; Dickmeiss, G.; Jiang, H.; Albrecht, L.; Jørgensen, K. A. *Acc. Chem. Res.* **2012**, *45*, 248−264. (k) Hernandez, J. G.; Juaristi, E. *Chem. Commun.* **2012**, *48*, 5396−5409. (l) Melchiorre, P. *Angew. Chem., Int. Ed.* **2012**, *51*, 9748−9770.

(2) For selected reviews, see: (a) Wennemers, H. *Chem. Commun.* **2011**, *47*, 12036−12041. (b) Freund, M.; Tsogoeva, S. B. In *Catalytic Methods in Asymmetric Synthesis: Advanced Materials, Techniques, and Applications*; Gruttadauria, M., Giacalone, F., Eds.; Wiley: Hoboken, NJ, 2011; pp 529−578. (c) Davie, E. A. C.; Mennen, S. M.; Xu, Y.; Miller, S. J. *Chem. Rev.* **2007**, *107*, 5759−5812. (d) Miller, S. J. *Acc. Chem. Res.* **2004**, *37*, 601−610.

(3) For selected reviews and recent reports on combinatorial methods for catalyst discovery and development, see: (a) Lichtor, P. A.; Miller, S. J. *Nat. Chem.* **2012**, *4*, 990−995. (b) Lichtor, P. A.; Miller, S. J. *ACS Comb. Sci.* **2011**, *13*, 321−326. (c) Revell, J. D.; Wennemers, H. *Top. Curr. Chem.* **2007**, *277*, 251−266. (d) Revell, J. D.; Wennemers, H. *Curr. Opin. Chem. Biol.* **2007**, *11*, 269−278. (e) Hechavarría Fonseca, M.; List, B. *Curr. Opin. Chem. Biol.* **2004**, *8*, 319−326. (f) Wennemers, H. Combinatorial Methods for the Discovery of Catalysts. In *Highlights in Bioorganic Chemistry*; Schmuck, C., Wennemers, H., Eds.; Wiley-VCH: Weinheim, Germany, 2004; pp 436−445. (g) Berkessel, A. *Curr. Opin. Chem. Biol.* **2003**, *7*, 409−419.

(4) Zhu, J.; Bienyamé, H. *Multicomponent Reactions*; Wiley-VCH, Weinheim, Germany, 2005.

(5) (a) Brauch, S.; van Berkel, S. S.; Westermann, B. *Chem. Soc. Rev.* **2013**, *42*, 4948−4962. (b) Dömling, A.; Wang, W.; Wang, K. *Chem. Rev.* **2012**, *112*, 3083−3135. (c) Ruijter, E.; Scheffelaar, R.; Orru, R. V. A. *Angew. Chem., Int. Ed.* **2011**, *50*, 6234−6246. (d) Wessjohann, L. A.; Rivera, D. G.; Vercillo, O. E. *Chem. Rev.* **2009**, *109*, 796−814. (e) El Kaïm, L.; Grimaud, L. *Tetrahedron* **2009**, *65*, 2153−2171.

(6) (a) Ruijter, E.; Orru, R. V. A. *Drug Discovery Today: Technol.* **2013**, *10*, 15−20. (b) Slobbe, P.; Ruijter, E.; Orru, R. V. A. *Med. Chem. Commun.* **2012**, *3*, 1189−1218. (c) Akritopoulou-Zanze, I. *Curr. Opin. Chem. Biol.* **2008**, *12*, 324−331. (d) Hulme, C.; Gore, V. *Curr. Med. Chem.* **2003**, *10*, 51−80.

(7) Touré, B. B.; Hall, D. G. *Chem. Rev.* **2009**, *109*, 4439−4486.

(8) (a) Wiesner, M.; Revell, J. D.; Wennemers, H. *Angew. Chem., Int. Ed.* **2008**, *47*, 1871−1874. (b) Wiesner, M.; Revell, J. D.; Tonazzi, S.; Wennemers, H. *J. Am. Chem. Soc.* **2008**, *130*, 5610−5611. (c) Wiesner, M.; Neuburger, M.; Wennemers, H. *Chem.—Eur. J.* **2009**, *15*, 10103−10109. (d) Wiesner, M.; Upert, G.; Angelici, G.; Wennemers, H. *J. Am. Chem. Soc.* **2010**, *132*, 6−7. (e) Duschmalé, J.; Wennemers, H. *Chem.—Eur. J.* **2012**, *18*, 1111−1120. (f) Duschmalé, J.; Wiest, J.; Wiesner, M.; Wennemers, H. *Chem. Sci.* **2013**, *4*, 1312−1318. For similar organocatalyst design, see: (g) Ramasastry, S. S. V.; Albertshofer, K.; Utsumi, N.; Barbas, C. F., III. *Org. Lett.* **2008**, *10*, 1621−1624. (h) Lipshutz, B. H.; Ghorai, S. *Org. Lett.* **2012**, *14*, 422−425. (i) Vishnumaya, M. R.; Singh, V. K. *J. Org. Chem.* **2009**, *74*, 4289−4297. (j) Schwab, R. S.; Galetto, F. Z.; Azeredo, J. B.; Braga, A. L.; Ludtke, D. S.; Paixão, M. W. *Tetrahedron Lett.* **2008**, *49*, 5094−5097.

(9) (a) Revell, J. D.; Gantenbein, D.; Krattiger, P.; Wennemers, H. *Biopolymers* **2006**, *84*, 105−113. (b) Revell, J. D.; Wennemers, H. *Tetrahedron* **2007**, *63*, 8420−8424. (c) Revell, J. D.; Wennemers, H. *Adv. Synth. Catal.* **2008**, *350*, 1046−1052. (d) Messerer, M.; Wennemers, H. *Synlett* **2011**, 499−502.

(10) (a) Dömling, A.; Ugi, I. *Angew. Chem., Int. Ed.* **2000**, *39*, 3168−3210. (b) Marcaccini, S.; Torroba, T. *Nat. Protoc.* **2007**, *2*, 632−639. (c) Ugi, I.; Meyr, R.; Fetzer, U.; Steinbrücker, C. *Angew. Chem.* **1959**, *71*, 386.

(11) (a) Wessjohann, L. A.; Rhoden, C. R. B.; Rivera, D. G.; Vercillo, O. E. *Top. Heterocycl. Chem.* **2010**, *23*, 199−226. (b) Gulevich, A. V.; Zhdanko, A. G.; Orru, R. V. A.; Nenajdenko, V. G. *Chem. Rev.* **2010**, *110*, 5235−5331. (c) Dömling, A. *Chem. Rev.* **2006**, *106*, 17−89. (d) Wessjohann, L. A.; Andrade, C. K. Z.; Vercillo, O. E.; Rivera, D. G. *Targets Heterocycl. Syst.* **2006**, *10*, 24−53. (e) Ugi, I.; Marquarding, D.; Urban, R. In *Chemistry and Biochemistry of Amino Acids, Peptides and Proteins*; Weinstein, B., Ed.; Marcel Dekker: New York, 1982; pp 246−289.

(12) Znabet, A.; Ruijter, E.; de Kanter, F. J. J.; Köhler, V.; Helliwell, M.; Turner, N. J.; Orru, R. V. A. *Angew. Chem., Int. Ed.* **2010**, *49*, 5289−5292.

(13) For examples of peptide−peptoid hybrids, see: (a) Rivera, D. G.; León, F.; Concepción, O.; Morales, F. E.; Wessjohann, L. A. *Chem.—Eur. J.* **2013**, *19*, 6417−6428. (b) Brandt, W.; Herberg, T.; Wessjohann, L. *Biopolymers (Pept. Sci.)* **2011**, *96*, 651−668. (c) Olsen, C. A. *ChemBioChem* **2010**, *11*, 152−160. (d) Patch, J. A.; Kirshenbaum, K.; Seurynck, S. L.; Zuckermann, R. N.; Barron, A. E. In *Pseudo-peptides in Drug Discovery*; Nielsen, P. E., Ed.; Wiley-VCH: Weinheim, Germany, 2004; pp 1−30.

(14) The multicomponent approach of Orru and co-workers (ref 12) to a prolyl peptide catalyst encompasses the utilization of only one element of diversity, namely, the isocyanide, while N-protected D-proline and chiral 1-pyrrolines are used as fixed components. Consequently, such a seminal report may not be regarded as combinatorial.

(15) For selected reviews, see: (a) Chowdari, N. S.; Ramachary, D. B.; Barbas, C. F., III. *Synlett* **2003**, *12*, 1906−1909. (b) List, B. *Acc. Chem. Res.* **2004**, *37*, 548−557. (c) Dalko, P. I.; Moisan, L. *Angew. Chem., Int. Ed.* **2004**, *43*, 5138−5175. (d) Seayad, J.; List, B. *Org. Biomol. Chem.* **2005**, *3*, 719−724. (e) Tsogoeva, S. B. *Eur. J. Org. Chem.* **2007**, 1701−1716. (f) Zhang, Y.; Wang, W. *Catal. Sci. Technol.* **2012**, *2*, 42−53.

(16) (a) List, B.; Pojarliev, P.; Martin, H. J. *Org. Lett.* **2001**, *3*, 2423−2425. (b) Betancort, J. M.; Barbas, C. F., III. *Org. Lett.* **2001**, *3*, 3737−3740.

(17) (a) Moberg, C. *Angew. Chem., Int. Ed.* **2013**, *52*, 2160−2162. (b) Burés, J.; Armstrong, A.; Blackmond, D. G. *J. Am. Chem. Soc.* **2012**, *134*, 6741−6750. (c) Seebach, D.; Sun, X.; Sparr, C.; Ebert, M.-O.; Schweizer, W. B.; Beck, A. K. *Helv. Chim. Acta* **2012**, *95*, 1064−1078. (d) Patora-Komisarska, K.; Benohoud, M.; Ishikawa, H.; Seebach, D.; Hayashi, Y. *Helv. Chim. Acta* **2011**, *94*, 719−745. (e) Burés, J.; Armstrong, A.; Blackmond, D. G. *J. Am. Chem. Soc.* **2011**, *133*, 8822−8825.

(18) Hayashi, Y.; Gotoh, H.; Hayashi, T.; Shoji, M. *Angew. Chem., Int. Ed.* **2005**, *44*, 4212−4215.

(19) This a typical feature of short peptoids and peptide−peptoid hybrids. For example, see: Sui, Q.; Borchardt, D.; Rabenstein, D. L. *J. Am. Chem. Soc.* **2007**, *129*, 12042−12048.

(20) Seebach, D.; Golinski, J. *Helv. Chim. Acta* **1981**, *64*, 1413−1423.

(21) Barros, M. T.; Phillips, A. M. F. *Eur. J. Org. Chem.* **2007**, 178−185.

(22) Cheng, Y.-Q.; Bian, Z.; He, Y.-B.; Han, F.-S.; Kang, C.-Q.; Ning, Z.-L.; Gao, L.-X. *Tetrahedron: Asymmetry* **2009**, *20*, 1753−1758.

(23) Polak, E.; Ribiere, G. *Rev. Fr. Inf. Rech. Oper., Ser. Rouge* **1969**, *16*, 35.

(24) Halgren, T. A. *J. Comput. Chem.* **1996**, *17*, 490−519.

(25) (a) *MacroModel*, version 9.9; Schrödinger, LLC: New York, 2012. (b) Richards, N. G. J.; Guida, W. C.; Liskamp, R.; Lipton, M.; Caufield, C.; Chang, G.; Hendrickson, T.; Still, W. C. *J. Comput. Chem.* **1990**, *11*, 440−467.

(26) *Maestro*, version 9.3; Schrödinger, LLC: New York, 2012.

(27) http://www.schrodinger.com/scriptcenter (accessed Oct 1, 2013).

(28) (a) Manetti, C.; Fogliano, V.; Ritieni, A.; Santini, A.; Randazzo, G.; Logrieco, A.; Mannina, L.; Sagre, A. L. *Struct. Chem.* **1995**, *6*, 183−189. (b) Gouda, H.; Sunazuka, T.; Ui, H.; Handa, M.; Sakoh, Y.; Iwai, Y.; Hirono, A.; Omura, S. *Proc. Natl. Acad. Sci. U.S.A.* **2005**, *102*, 18286−18291. (c) Shao, J.; Tanner, S. W.; Thompson, N.; Cheatham, T. E., III. *J. Chem. Theory Comput.* **2007**, *3*, 2312−2334.

(29) (a) Zhao, Y.; Truhlar, D. G. *Theor. Chem. Acc.* **2008**, *120*, 215−241. (b) Zhao, Y.; Truhlar, D. G. *Acc. Chem. Res.* **2008**, *41*, 157−167.

(30) Frisch, M. J.; Trucks, G. W.; Schlegel, H. B.; Scuseria, G. E.; Robb, M. A.; Cheeseman, J. R.; Scalmani, G.; Barone, V.; Mennucci, B.; Petersson, G. A.; Nakatsuji, H.; Caricato, M.; Li, X.; Hratchian, H. P.; Izmaylov, A. F.; Bloino, J.; Zheng, G.; Sonnenberg, J. L.; Hada, M.; Ehara, M.; Toyota, K.; Fukuda, R.; Hasegawa, J.; Ishida, M.; Nakajima, T.; Honda, Y.; Kitao, O.; Nakai, H.; Vreven, T.; Montgomery, J. A., Jr.;

Peralta, J. E.; Ogliaro, F.; Bearpark, M.; Heyd, J. J.; Brothers, E.; Kudin, K. N.; Staroverov, V. N.; Kobayashi, R.; Normand, J.; Raghavachari, K.; Rendell, A.; Burant, J. C.; Iyengar, S. S.; Tomasi, J.; Cossi, M.; Rega, N.; Millam, N. J.; Klene, M.; Knox, J. E.; Cross, J. B.; Bakken, V.; Adamo, C.; Jaramillo, J.; Gomperts, R.; Stratmann, R. E.; Yazyev, O.; Austin, A. J.; Cammi, R.; Pomelli, C.; Ochterski, J. W.; Martin, R. L.; Morokuma, K.; Zakrzewski, V. G.; Voth, G. A.; Salvador, P.; Dannenberg, J. J.; Dapprich, S.; Daniels, A. D.; Farkas, Ö.; Foresman, J. B.; Ortiz, J. V.; Cioslowski, J.; Fox, D. J. *Gaussian 09*, revision B.1; Gaussian, Inc.: Wallingford, CT, 2009.

(31) Marenich, A. V.; Cramer, C. J.; Truhlar, D. G. *J. Phys. Chem. B* **2009**, *113*, 6378−6396.